Acta Cryst. (1999). A**55**, 533–542

Moiré patterns in electron microscopy with atomic focuser crystals

J. M. Cowley,[a]* Newton Ooi[a] and R. E. Dunin-Borkowski[b]

[a]*Department of Physics and Astronomy, Arizona State University, Tempe, AZ 85287-1504, USA, and* [b]*Center for Solid State Science, Arizona State University, Tempe, AZ 85287-1704, USA. E-mail: cowleyj@asu.edu*

(*Received 23 September 1998; accepted 12 November 1998*)

Abstract

The periodic array of very fine cross-overs formed at the exit face of a thin 'atomic focuser' crystal, illuminated by a parallel electron beam, may be used to form moiré patterns with a specimen crystal such that the structure of the specimen crystal may be derived with a resolution of better than 0.5 Å. Computer simulations of the moiré pattern formation have been made for the simple idealized case of two parallel gold-like lattices having a 10% difference in lattice constant. Moiré images are shown for the case of a small objective aperture in the viewing electron microscope such that the individual crystal lattices are not resolved and for a larger objective aperture for which the individual crystal lattices are resolved and the intensity is measured at the positions of the atoms of the atomic focuser crystal. The latter case confirms the viability of the scheme for ultra-high-resolution imaging of general specimens by use of a thin-crystal periodic atomic focuser, as previously proposed.

1. Introduction

The observation of moiré patterns in the electron microscopy of superimposed thin crystals is a well known phenomenon that achieved considerable prominence about forty years ago. At that time, the resolution capabilities of electron microscopes were not sufficient to allow the direct imaging of the periodicities of individual crystals except in the case of a few crystals having large lattice-plane periodicities (see Hirsch *et al.*, 1965). Applications of moiré imaging included the detection of dislocations and other defects in crystals. However, the discussions of the formation of moiré patterns using dynamical diffraction theory in the two-beam approximation (Hashimoto *et al.*, 1960; Cowley, 1959) showed that the intensity distributions of the moiré patterns do not necessarily reflect the forms of the crystal defects. In fact, the appearance of dislocation-like features in the moiré patterns may arise from variations of thickness or orientation of the crystals in the absence of any crystal defects.

It was shown, however, that a direct relationship between the intensity distribution in moiré patterns and the structures of the contributing crystals is possible for the case of very thin weakly scattering crystals (see, for example, Cowley & Moodie, 1959). For two crystals which are in axial orientations and which have a small difference in lattice spacings, or which have a small relative difference in orientation, double diffraction gives a regularly spaced array of spots close to the zero beam of the diffraction pattern. Imaging with this spot pattern gives a corresponding two-dimensionally periodic image with large periodicities in real space. When the weak-phase-object approximation (WPOA) is valid, it may be shown that the intensity distribution of this large-scale periodic moiré pattern is given by the convolution of one projected crystal structure with the projected crystal structure of the other, inverted through the origin. Then, if the structure of one of the crystals is known, the projected crystal structure of the other may be deduced. The effective resolution with which the structure of the unknown crystal may be deduced is little affected by the aberrations of the microscope but, for a sufficiently large magnification through the moiré formation, may be as small as a fraction of an ångström.

There are no known examples of the determination of a crystal structure by the use of moiré patterns in this way. It is not easy to form crystals so thin that the WPOA is valid when the incident beam is in an axial orientation. Also, it may be noted that the basis of the WPOA is that the amplitudes of the diffracted beams are very small compared with that of the zero beam. The amplitudes of the doubly diffracted beams that contribute to the moiré image must be much smaller still and the contrast of a moiré image that can be interpreted on the basis of the WPOA must be extremely small.

Hence, when the resolution limits of the available electron microscopes became sufficiently small to allow the direct imaging of the structures of many simple crystals, there seemed to be little point in attempting to make use of the moiré phenomena.

A possible basis for the revival of interest in moiré patterns as a means for the study of the structures of crystals with ultra-high resolution is given by the results of the many-beam dynamical diffraction calculations that have been made for crystals of moderate thickness in axial orientations, for example, by Fertig & Rose (1981), Marks (1985), Loane *et al.* (1988) and Dunin-Borkowski & Cowley (1999). It has been shown that

incident electrons may be channeled along rows of atoms aligned in the beam direction (Van Dyck & Op de Beeck, 1996) so that the exit wave forms a very sharp intense cross-over at the position of the exit atom of each atom row. The intensity and width of the wave along the axis of the atomic row vary periodically with crystal thickness, apart from absorption effects, and the periodicity depends on the atomic numbers and separations of the atoms along the rows.

The occurrence of the periodic array of very fine cross-overs, less than 0.5 Å in diameter, at the exit face of a crystal has been shown to provide a possible basis for the imaging of samples with ultra-high resolution in one of the schemes proposed for the application of 'atomic focusers' in transmission electron microscopy (Cowley *et al.*, 1997). In this scheme, a thin crystal is illuminated by a plane incident wave so that the array of very fine cross-overs formed at the atomic positions in the exit face is coherent. Then identical arrays of fine cross-overs are formed at the Fourier-image positions in the space following the crystal. The specimen is placed at one of these Fourier-image positions and is imaged by an electron microscope that has sufficient resolution to allow the periodicity of the atomic focuser crystal to be resolved. The image formed by such a microscope shows a pattern of spots and each spot represents the intensity formed when one of the very fine probes is transmitted through the specimen. The array of very fine probes may be scanned across the specimen simply by tilting the incident-beam direction through small angles. Then the intensity distribution of an image with resolution better than 0.5 Å may be deduced by correlation of the images formed with different incident-beam tilts.

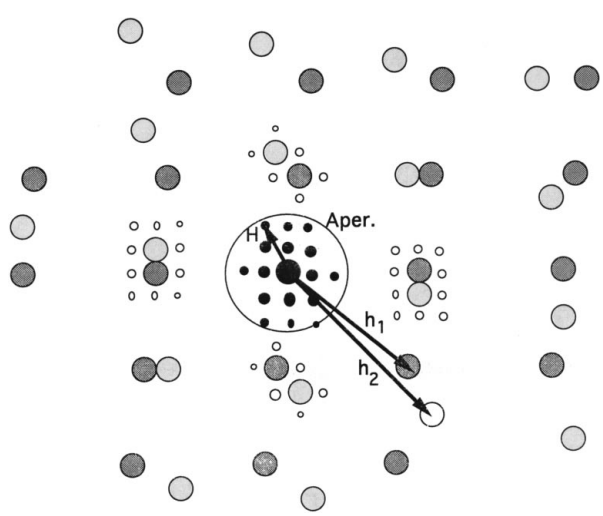

Fig. 1. Diagram of the diffraction patterns for two crystals (large circles) and the double-diffraction spots (small circles). The objective aperture used to obtain the moiré pattern in the electron microscope image with the individual lattices not resolved is indicated.

In such a scheme, special considerations apply if the specimen is also a thin single crystal. If the periodicity of the specimen crystal differs by a small amount (preferably less than about 10%) from that of the atomic focuser crystal or if the directions of the axes differ by a few degrees, there is a small relative translation of the unit-cell origins of the two crystals in adjacent unit cells. There is a coincidence of the origins of the unit cells at the points of a large-period lattice; *i.e.* a moiré pattern is formed. From one electron micrograph taken with a microscope of normal resolution, the structure of the specimen crystal can be deduced with an effective resolution of a small fraction of an ångström.

In this paper, we explore, by means of computer simulations, the possibilities for obtaining useful images of moiré patterns from superimposed crystals of reasonable thickness as a basis for the deduction of the structures of thin crystals with ultra-high resolution. We also report preliminary experimental observations on the formation of such images.

2. The formation of moiré patterns

For two superimposed thin crystals, the diffraction pattern formed in the back-focal plane of an electron-microscope objective lens contains the primary diffraction spots from each of the two crystals. It also contains the doubly diffracted spots from the electrons scattered from the first crystal, with diffraction vector $\mathbf{h}_1$ $(= h_1\mathbf{a}_1^* + k_1\mathbf{b}_1^*)$, and then from the second crystal with diffraction vector $\mathbf{h}_2$ $(= h_2\mathbf{a}_2^* + k_2\mathbf{b}_2^*)$, where the h, k are integers and the $\mathbf{a}^*$, $\mathbf{b}^*$ are the unit-cell reciprocal-space vectors for the projections of the crystal structures. If the end-points of the vectors $\mathbf{h}_1$ and $\mathbf{h}_2$, drawn from the origin, are close together (*i.e.* if the crystal lattice periodicities are almost the same or if the crystal axes are in slightly different directions), the vectors $\mathbf{H} = \mathbf{h}_1 - \mathbf{h}_2$ define a lattice of points around the origin, as well as around all of the sets $\mathbf{h}_1$ and $\mathbf{h}_2$, as suggested in Fig. 1. If an objective aperture isolates only the set of points $\mathbf{H}$ around the origin, which has a one-to-one correspondence with the set $\mathbf{h}_1$ or $\mathbf{h}_2$, the image formed has a periodicity reciprocal to the spacings of the $\mathbf{H}$ set and so shows a periodicity much greater than that of either lattice, *i.e.* a moiré pattern.

In the ideal case, the objective aperture, which defines the resolution of the electron microscope, has a radius that is less than half the magnitude of the smallest of the $\mathbf{a}^*$, $\mathbf{b}^*$ vectors; the magnitude of the first-order $\mathbf{H}$ vectors is so much smaller than the objective aperture that the image includes many orders of the double-diffraction spots around the origin. The moiré image is formed with real-space periodicities so much larger than those of the crystal lattices that there is sufficient magnification of the structural detail to allow an effective resolution of the detail within the image. In the simplest case, when the moiré pattern is given by the superposition of crys-

tals having identical lattice dimensions, rotated with respect to each other by only a few degrees, or when the axes of the two crystals are parallel and differing in length with a ratio only slightly different from unity, the moiré pattern shows an enlarged image of the unit cells. The amplitude of the doubly scattered beam corresponding to the nth vector of the set $\boldsymbol{H}$, given by

$$\boldsymbol{H}_n = H_n(\mathbf{a}^*_{1n} - \mathbf{a}^*_{2n}) + K_n(\mathbf{b}^*_{1n} - \mathbf{b}^*_{2n}) = H\mathbf{A}^* + K\mathbf{B}^*,$$

where the subscripts 1 and 2 refer to the two crystals, is given by the Fourier transform of the product of the transmission functions of the two crystals. So the amplitude of the moiré image function is

$$\psi_m(\mathbf{r}) = \sum_n \Psi_1(\mathbf{h}_{1n})\Psi_2(-\mathbf{h}_{2n}) \exp[2\pi i(\mathbf{H}_n \cdot \mathbf{r})], \qquad (1)$$

where the summation is limited to the $\boldsymbol{H}_n$ points within the aperture. In the weak-phase-object approximation, the diffracted amplitudes are written $\Psi(\mathbf{u}) = \delta(\mathbf{u}) - i\sigma\Phi(\mathbf{u})$, where $\Phi(\mathbf{u})$ is the Fourier transform of the projected potential function, $\varphi(\mathbf{r})$. Equation (1) then gives the amplitude of the moiré pattern as

$$\psi_m(\mathbf{R}) = 1 - \sigma^2[\varphi_1(\mathbf{R}) * \varphi_2(-\mathbf{R})] * \sum_{m,n} \delta(\mathbf{R} - m\mathbf{A} + n\mathbf{B}), \qquad (2)$$

where the two-dimensional vector $\mathbf{R}$ refers to the scale of the moiré pattern which is periodic with axial vectors $\mathbf{A}$ and $\mathbf{B}$. The intensity distribution of the moiré pattern, given by the square of (2), is the same except for a factor of 2 in the second term since the $\sigma\varphi$ terms are assumed to be small.

For this ideal case, it is clear that, for identical crystals, the moiré pattern gives the autocorrelation function, or Patterson function, of the projected potential function. For two crystals of different structure, if one crystal structure is known, the other can be deduced. The resolution that may be achieved in the determination of this structure is not limited by the aberrations of the electron microscope but is governed by the number of double-diffraction spots falling within the aperture and so depends on the differences in the lattice vectors $\mathbf{h}_1$ and $\mathbf{h}_2$ for the two crystals.

It may be noted that, because for the WPOA the product $\sigma\varphi$ is assumed to be very small, the contrast of the moiré pattern must be extremely small. Appreciable contrast in the moiré pattern can be obtained only if the strict requirements of the WPOA are relaxed, in which case the simple intensity expression from (2) is no longer valid. However, it has been pointed out (Cowley, 1976) that, if the phase-object approximation (POA, the projection approximation for thin crystals) is valid, the autocorrelation function has peaks in the correct position and intensities perturbed in a nonlinear but monotonic fashion for an appreciable range of $\sigma\varphi$ maximum values. It was suggested that the crystal thicknesses for which this applies, for medium-weight elements, may be as great as a few nm for electrons in the usual energy range, giving observable levels of contrast.

The many-beam dynamical diffraction calculations have suggested that for monoatomic crystals of simple structure in axial orientations, with thicknesses as great as several tens of nm, the channeling of electrons along the rows of atoms may give a periodic array of beams of very small cross section at the exit surface of the crystal. In particular, Dunin-Borkowski & Cowley (1999) and Sanchez & Cowley (1998) have shown that, for simple metal crystals in axial orientation, the peaks of intensity at the ends of the atom rows may have full widths at half-height of less than 0.03 nm and that these peaks, to a good approximation, have uniform phase relative to a flat background. Such periodic exit wave functions from a first crystal would seem to be ideal for forming moiré patterns. To a good approximation, $\sigma\varphi_1(\mathbf{R})$ in (2) may be replaced by $\delta(\mathbf{R})$ so that the structure of the second, superimposed, crystal may be imaged directly with very high resolution.

One obvious difficulty with this idea is that there are very few crystals of unknown structure that have unit cells of size comparable with those for the simple monoatomic crystals for which the atomic focuser effect gives a well defined uniform periodic set of sharp intensity maxima. Under these circumstances, the formation of the moiré pattern is more readily discussed in terms of the real-space coincidences of atom positions in the projections of the two crystals.

For the simple case that the focuser and specimen crystals have dimensions that are close together, it is seen that, if the atomic rows in the two crystals coincide at one position, they will coincide again, within a tolerance limit of, say 0.1 Å, at a regularly spaced set of points which define the moiré unit-cell axes, defined in terms of the axes of the unit cell of the first crystal as $\mathbf{A} = n\mathbf{a}_1$, $\mathbf{B} = m\mathbf{b}_1$, where n and m are integers. Then for an atom at a position given by fractional coordinates x, y, there will be a coincidence, giving a peak in the moiré image unit cell, at the position $x\mathbf{A}$, $y\mathbf{B}$.

If the specimen crystal has a unit cell that is considerably larger than that of the focuser crystal, the periodic set of sharp intensity maxima from the first crystal samples a set of points within the second-crystal unit cell. Within an adjacent unit cell of the second crystal, the set of points sampled is shifted with respect to those in the first unit cell. Within the large-scale periodicities of the moiré unit cell, the set of intensity points from the first crystal samples any particular point of the second crystal in at least one of the unit cells of the second crystal within the required accuracy of 0.1 Å or less. This is so unless, by chance, the unit-cell dimensions of the two crystals are in the ratio of two small integers. Then the set of points sampled within the second-crystal unit

cell may be limited to a few widely separated lines of points.

In general, there is no obvious relationship between the position within the moiré unit cell where a peak appears and the position of the corresponding atom within the specimen crystal unit cell, but these positions can be related by use of a relatively simple algorithm, given the unit-cell dimensions. The correlation of intensity peaks in the TEM image of the moiré pattern with the atom positions follows much the same principles as in the corresponding form of the atomic focuser scheme in which the set of sharp intensity maxima from the first crystal is translated across the specimen by means of a tilt of the incident-beam direction.

In the original discussions of moiré-pattern formation (*e.g.* Cowley & Moodie, 1959), it was assumed that an objective aperture is inserted to remove all diffraction spots given by the two crystals separately and to allow only the doubly diffracted spots around the zero beam to contribute to the image. The contrast of the moiré-pattern image is necessarily then very small. When an atomic focuser crystal of appreciable thickness is used, the wave function incident on the specimen crystal has very high contrast since it consists of high sharp maxima on a low background. With the same small objective aperture, the contrast of the moiré pattern can then be close to the contrast for a normal TEM image of the specimen crystal.

Even greater contrast may be achieved in the moiré image if, as in the proposed atomic focuser scheme, the TEM instrument used to form the final image has sufficient resolution to resolve the periodicity of the first focuser crystal, and the intensities in the image are recorded only at the positions of the images of the atom rows of the first crystal.

We report here, initially, the results of computer simulations for a very simple model case of superimposed crystals in order to demonstrate clearly the characteristics of the moiré pattern and to indicate the levels of resolution and contrast that may be achieved in ideal situations.

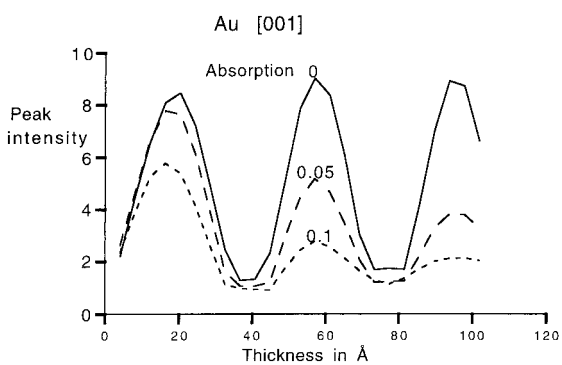

Fig. 2. Intensities of the sharp intensity peaks along the rows of atoms for Au [001] as a function of crystal thickness for the absorption factor (imaginary part of the scattering factor) equal to 0, 0.05 and 0.10 of the real part.

3. Simulations for gold-like crystals

When a coherent plane wave of 200 keV electrons illuminates a gold crystal in [001] orientation, the electrons are channeled along the atom rows. The wave amplitude and intensity form sharp peaks at the centers of the rows and are almost constant in the regions between the rows. The intensities of the peaks vary almost sinusoidally with distance along the rows if absorption effects are neglected.

With a reasonable absorption function introduced, this near-periodic variation is damped so that the second maximum is reduced to about half the value of the first. Fig. 2 shows the variations of the peak intensity calculated on the assumption of an imaginary part of the scattering factor equal to 0.1 and 0.05 of the real part. According to Renard *et al.* (1971), this fraction should probably be taken as about 0.07. With no Debye–Waller factor applied, the periodicity of the intensity variation

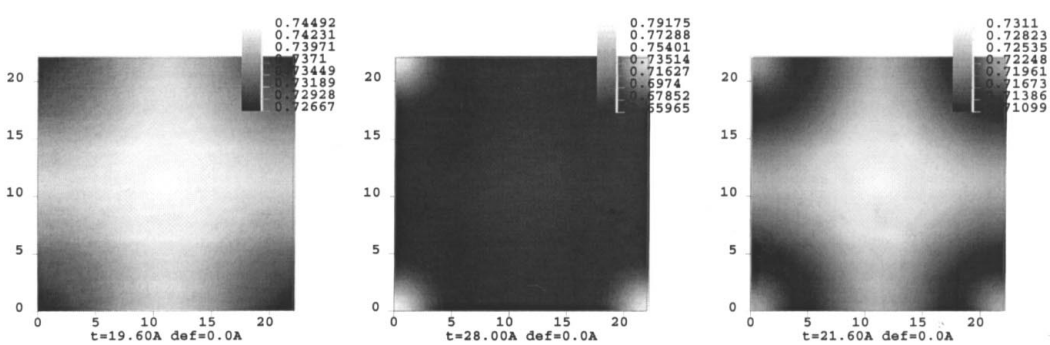

(*a*) (*b*) (*c*)

Fig. 3. Moiré patterns calculated for a small aperture (radius 0.25 Å^{-1}) with atoms coinciding at the origin (dimensions in Å), for (*a*) first crystal 17.6 Å; second crystal 2 Å; negative contrast; (*b*) first crystal 22 Å; second crystal 6 Å; sharp peak with positive contrast; (*c*) first crystal 17.6 Å; second crystal 4 Å; low, mixed contrast.

along the rows is about 46 Å (Sanchez & Cowley, 1998); with an appropriate D–W factor, the periodicity is 57 Å (Dunin-Borkowski & Cowley, 1999).

The width of the intensity peaks is about 0.25 Å except near the intensity minima, where the peaks become broad and the incident-beam amplitudes are almost recovered (see Fig. 2). The phases of electron waves across the peaks are almost constant. The phase difference relative to the background varies almost linearly with thickness, becoming equal to multiples of 2π at the positions of minimum peak intensity.

Simulation of moiré patterns have been made using the *CERIUS* software. The electron beam is considered to pass through two gold-like crystals having parallel axes but with unit-cell dimensions differing by 10%. The first crystal has gold atoms on a f.c.c. lattice with $a_0 = 4.4$ Å and the second crystal is the same except that $a_0 = 4.0$ Å. Since, in projection, the unit-cell dimensions are halved, the calculations are made for a superlattice 22 Å square and, for convenience in computing, it is assumed in each case that the f.c.c. lattice is replaced by a simple cubic lattice with half the unit-cell dimensions and half-occupancy of gold atoms at all lattice sites. With these assumptions, the form and periodicity of the intensity peaks along the atom rows are much the same as for normal Au (for which $a_0 = 4.08$ Å). In the real-space picture of the situation, it can be considered that in this case the periodic set of sharp intensity maxima from the first crystal samples the unit cell of the second crystal at intervals of 0.22 Å.

In order to simulate the formation of moiré patterns under the conditions usually considered, the exit wave from the second crystal is assumed to be viewed with a transmision electron microscope (TEM) with an objective aperture radius equal to about half the distance of the primary diffraction spots from the origin, namely 0.25 $Å^{-1}$, so that the periodicities of the individual crystals are not resolved. For the TEM, the defocus and C_s are assumed to be zero.

Calculations made for various thicknesses of the two crystals are illustrated in Fig. 3. In Fig. 3(*a*), there is a dark peak at the atom position at the origin (negative contrast), with about 3% contrast [as measured by $(I_{max} - I_{min})/(I_{max} + I_{min})$] and a half-width of about 3 Å, corresponding to a half-width of about 0.3 Å relative to the second-crystal unit cell. In Fig. 3(*b*), a much more common situation, there is a bright peak at the origin atom position (positive contrast) with about 20% contrast and a half-width of about 2 Å, corresponding to a full width, or an effective resolution, of about 0.4 Å relative to the second crystal unit-cell dimensions. Between these images, there are moiré images of very low contrast and poorly defined peaks, as in Fig. 3(*c*). As indicated by the gray scales in these images, the contrast has been expanded in each case so that the range from black to white corresponds to the range from minimum to maximum intensity.

In Fig. 4(*a*), the contrast of the origin peak is plotted for several thicknesses of the second crystal as a function of the thickness of the first crystal. In Fig. 4(*b*), the corresponding widths of the peaks are plotted. Because the widths are very much the same for all thicknesses of the second crystal, the curves for different thicknesses are not distinguished. The minimum peak half-width of about 2 Å in the moiré pattern, implying an effective resolution of about 0.4 Å in the imaging of the specimen crystal, is probably determined in this case by the size of the objective aperture rather than by the sharpness of the cross-overs coming from the focuser crystal.

It is seen that the contrast values for different thicknesses of the second crystal, up to 10 Å (2.5 gold atoms), increase almost linearly with thickness. As the first-crystal thickness increases, the contrast values vary almost sinusoidally, following the same periodicity as for the transmission through a single crystal (Fig. 2). For very small thicknesses of the first crystal, and again after one periodicity, the contrast is low and negative. With increase in the first-crystal thickness, the contrast reaches about 25% and is positive. The resolution of the

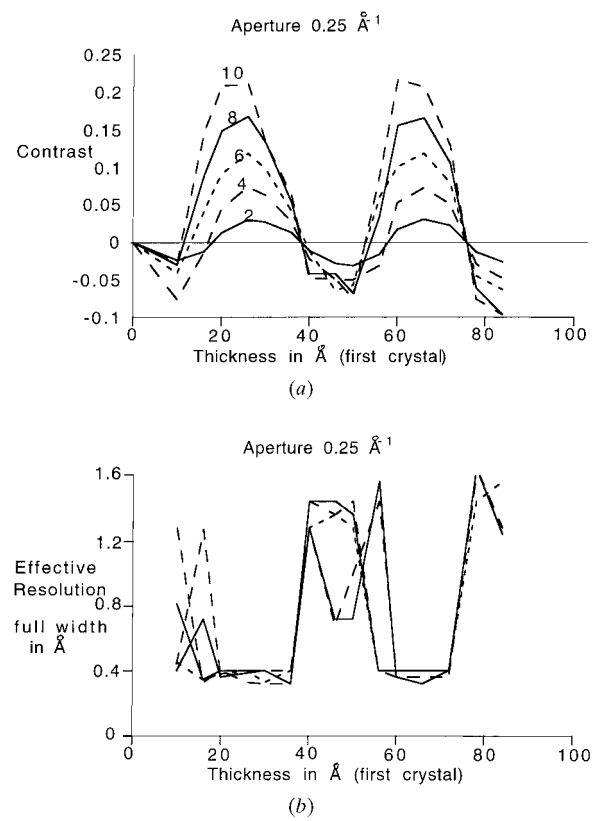

Fig. 4. Variation of (*a*) contrast of the peak in the moiré pattern formed with a small aperture, and (*b*) peak width, referred to the second crystal lattice, for various thicknesses (indicated on the graphs, in Å) of the second crystal as functions of the thickness of the first crystal. In (*b*), the curves overlap and are not readily distinguished.

peaks in the moiré pattern, referred to the dimensions of the individual unit cells of the second crystal, is poor, with peak half-widths of more than 0.4 Å when the contrast is low but, for all the regions of high contrast, the peak half-width is about 2 Å, suggesting an effective resolution for the specimen crystal of about 0.4 Å.

In order to simulate the formation of moiré images formed under the conditions of the atomic focuser

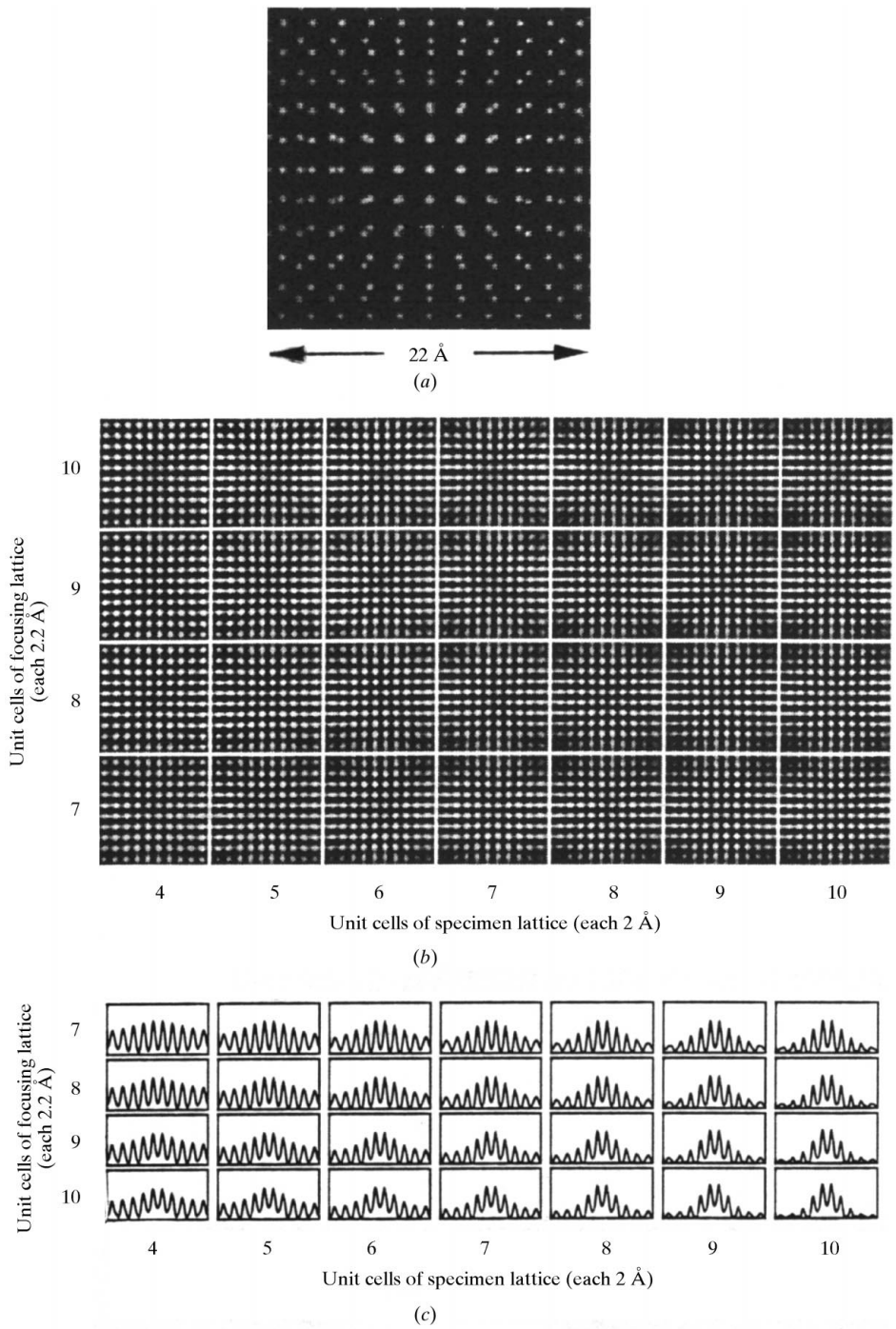

Fig. 5. (*a*) The superposed projected potential distributions of the two gold-like crystals, with the atoms of the two crystals coinciding at the center. (*b*) Some typical calculated moiré images of superimposed crystals for a range of thicknesses of the first crystal from 15.4 to 22 Å and for thicknesses of the second crystal from 8 to 20 Å, for defocus −408 Å and aperture radius 0.51 $Å^{-1}$. (*c*) Intensity distributions along lines through the centers of the images of (*b*).

scheme discussed above, the images are calculated for the same system but with an objective aperture radius of 0.51 Å^{-1}. This simulates the conditions that may be achieved with a present-day TEM having a resolution of better than 2 Å for 200 keV electrons and with an aperture large enough to allow the primary diffraction spots from the individual crystals to contribute to the image. A representative C_s value of 0.5 mm is chosen, the imaginary contribution to the structure factor is assumed to be 0.07 of the real part, a Debye–Waller factor of 0.62 is assumed, and the moiré images are calculated for zero defocus and for the Scherzer optimum defocus of −408 Å. In this case, the superimposed projections of the single-layer structures of the two crystals are as shown in Fig. 5(*a*), with the origin point, where the atoms of the two structures coincide, at the middle of the 22 Å-square unit cell. Typical images under these conditions are shown in Fig. 5(*b*). In these images, the periodicity of the first crystal is clearly visible. The intensities are measured only at the positions of the atoms of the first crystal which often appear as dark spots. Line scans such as those of Fig. 5(*c*) are made along the axial and diagonal directions through the central origin point of the simulated moiré unit cells. The intensities at the first-crystal atom positions are measured and plotted in curves to allow the contrast and resolution figures to be determined.

Fig. 6 shows the variation of contrast and peak width, plotted for various thicknesses of the second crystal, as a function of the thickness of the first crystal. The data refer in this case to the widths and contrast of only the small bright peaks at the central origin position. For small thicknesses, the main feature of the image is often a rather broad dark spot (negative contrast) at the origin (*cf.* Fig. 3*a*) but, with increasing thickness, a small bright spot develops within this broad dark spot (*cf.* Fig. 3*c*) and increases in intensity until, when the combined thickness of the two crystals exceeds about 30 Å, it dominates the whole intensity distribution (*cf.* Fig. 3*b*).

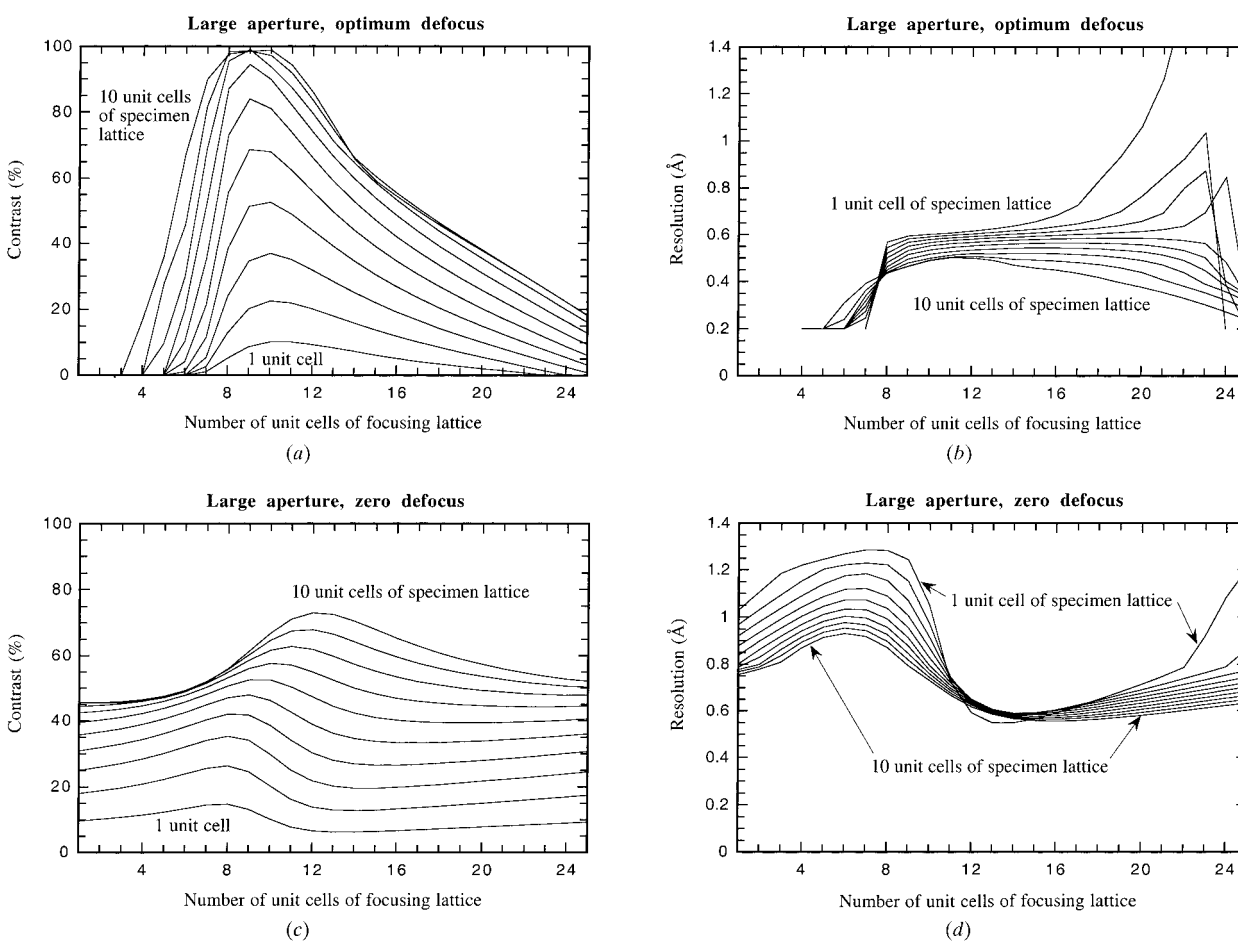

Fig. 6. Variations of contrast (*a*), (*c*) and effective resolution (*b*), (*d*) as functions of thickness of the first crystal (2.2 Å for each unit cell) for various thicknesses of the second crystal (from 0.5 to 5.0 gold atoms) for large aperture (0.51 Å^{-1}); for the optimum-defocus condition (*a*), (*b*) and the in-focus condition (*c*), (*d*) derived from the images of Fig. 5.

It is seen that the variations of contrast and effective resolution for the large-aperture simulations follow those for the small-aperture moirés of Fig. 4. The effective resolution values are much the same, the resolution referred to the specimen-crystal unit-cell dimensions being as small as 0.4 Å for the high-contrast thicknesses. The contrast shown in the resulting plots of Figs. 6(*a*) and 6(*c*) is considerably greater than for the small-aperture case of Fig. 4, especially for the optimum defocus case for which the contrast can approach 100%. For a single gold atom (two unit cells or 4 Å thickness), the contrast can be greater than 20%. As in the small-aperture case, the contrast increases initially almost linearly with the thickness of the second crystal. The resolution and contrast both become poor for the thicknesses around 55 Å (25 unit cells), which corresponds to the periodicity of the peak intensity variation along the atom rows of the focuser crystal.

In all the above simulations, it has been assumed that there is no space between the two crystals forming the moiré pattern. In practice, it is possible that the two crystals may be separated by a small distance with a layer of vacuum or of some light-atom material such as absorbed gas molecules or carbonaceous contamination between them. For one particular case, with a focusing crystal of thickness 33 Å, a specimen crystal of thickness 10 Å and a small aperture, the contrast of the peak in the moiré image has been calculated for various spacings between the crystals. Fig. 7 shows that, after a slight increase, the contrast decreases to about half for a separation of 20 Å.

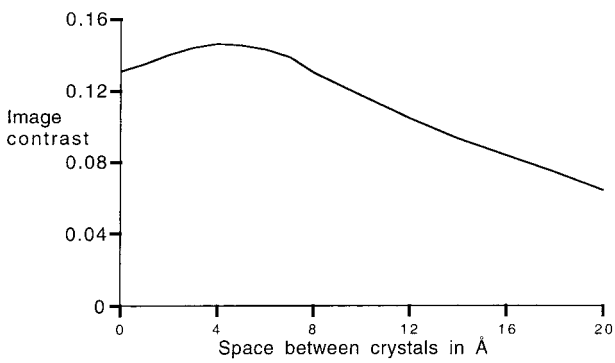

Fig. 7. Contrast of the moiré image, obtained with the small aperture, as a function of crystal separation for the particular case of a first crystal 33 Å thick and a second crystal 10 Å thick.

4. Experimental two-dimensional moiré patterns

It is known (*e.g.* Cowley, 1967) that bismuth oxychloride, BiOCl, can form very thin uniform crystals when precipitated from a solution of $BiCl_3$ in HCl by the addition of water. The BiOCl crystals are tetragonal with unit-cell axes $a = 3.88$ and $c = 7.35$ Å. When a film of Ag is evaporated on such crystals, heated to 570 K, some Ag crystals grow epitaxically on the BiOCl. Many moiré patterns appear in the electron-microscope images and some show two-dimensional intensity distributions as in the STEM images of Fig. 8. Nano-diffraction patterns from the regions of the moiré patterns suggest that the [110] axis of the Ag may be parallel to the [100] or [001] axis of the BiOCl. While detailed simulations for these images have not been carried out, several features of the images are of interest.

It may be noted that, especially in the image of Fig. 8(*a*), there is periodically recurring detail on a scale of about one fifth of the moiré unit-cell repeat distances. The limit on the fineness of the detail may be set by the use, in this case, of an aperture giving a nominal resolution of about 7 Å. This suggests that, when referred to the unit-cell dimensions of the specimen crystal, information is present corresponding to a resolution of less than one fifth of the periodicities in the projected unit

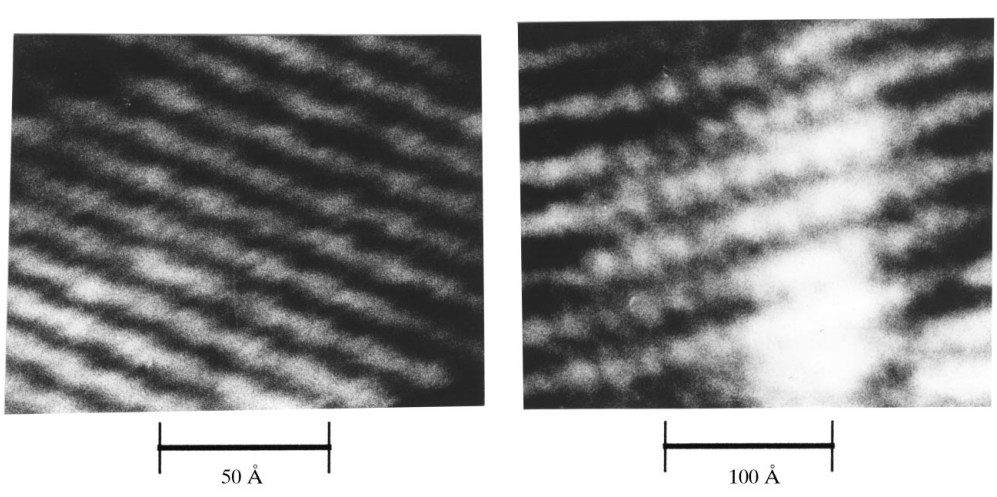

Fig. 8. Two-dimensional moiré patterns from Ag on BiOCl.

cell (about 2 Å), which would imply an effective resolution limit of much less than 1 Å.

5. Discussion and conclusions

The simulations that have been made for the idealized case of two superimposed parallel gold-like structures, differing only in unit-cell parameters, and the very limited experimental observations made to date, confirm that observation of moiré patterns should allow the determination of the structure of an unknown specimen crystal with an effective resolution approaching 0.4 Å. In order to achieve such a resolution with good contrast, it is necessary that the first, focusing, crystal should have a thickness in one of the ranges giving the maximum focusing effect but, as is evident from Figs. 4 and 6, these ranges are quite broad and recur with increasing thickness so that this requirement is not very restrictive. The contrast of the moiré image may be high for suitable specimen thicknesses, suggesting the possibility of deriving images for crystals having a wide range of projected potential peaks resulting from the presence of atoms with a wide range of atomic number.

It is also a requirement that both the focusing crystal and the specimen crystal should be in a principal orientation so that the electrons travel parallel to rows of atoms. This may be achieved if one crystal is grown epitaxically on the other. Some complications could arise if, in the course of the epitaxic growth, one of the lattices is relaxed near the surface to give a closer fit to the other. If the relaxation involves only one or two layers of atoms, the effect on the moiré pattern may be small. On the other hand, since good contrast may be given by a specimen consisting of only a few layers of relatively heavy atoms on the focuser crystal, the observations of moiré patterns may serve for the investigation of the initial form of crystalline layers grown epitaxically on crystal surfaces.

In our simulations, it has been assumed that the focuser and specimen crystals are of uniform thickness and orientation. The practical requirements are that these uniformities should extend over regions of diameter greater than the dimensions of the moiré unit cell, normally of the order of 100 Å or less. It is evident from Figs. 4, 6(*a*) and 6(*c*) that, for the thicknesses of the focuser crystal giving maximum contrast, a variation of thickness of 5 to 10 Å within this region gives no appreciable effect and, for thin specimens, the contrast is approximately proportional to the thickness. It is estimated that no appreciable effect on the moiré contrast should be noticeable for variations of orientation of a few degrees within the 100 Å areas.

It is suggested by Fig. 7 that, for crystals superimposed but separated by a gap of vacuum or of light-atom material (such as absorbed gas atoms or contamination), the moiré contrast may not be greatly affected unless the gap is greater than about 20 Å. For much greater separations, it may be possible to take advantage of the repetition of the conditions for useful moiré formation occurring at the Fourier-image distances from the focuser crystal.

For the experimentally feasible case that the focuser crystal is monoatomic and has small projected unit-cell dimensions and the specimen crystal is of more complicated structure with relatively large unit-cell dimensions, complications arise in that the information regarding the structure of the specimen crystal may be distributed over a large number of unit cells. A simple algorithm may be developed to determine the correlation between the positions of the intensity maxima in the moiré pattern and the positions of the atoms in the specimen crystal. However, the computer simulations required to predict the intensity distributions may be more complicated in that they would have to be repeated for a number of specimen-crystal unit cells having different positions relative to the focuser unit-cell origin.

The computer simulations reported here for the case of the large aperture, allowing the periodicity of the focuser crystal to be resolved, may be considered as a confirmation of the validity of the atomic focuser imaging scheme proposed by Cowley *et al.* (1997) for imaging of general specimens with ultra-high resolution by use of an atomic focuser crystal producing a periodic array of fine cross-overs, which is translated over the specimen by tilting the incident beam. It is concluded that high-contrast images having resolutions of the order of 0.4 Å may be derived by correlating the intensity measurements at the periodic set of points corresponding to the atom rows of the focuser crystal in images recorded with a microscope having just sufficient resolution to image the focuser crystal lattice (see Cowley *et al.*, 1998).

The experimental two-dimensional moiré images achieved so far are of a very primitive preliminary nature, but are sufficient to suggest that effective resolutions in the predicted range may be realized.

This research made use of the facilities of the ASU Center for High Resolution Electron Microscopy. We gratefully acknowledge the assistance of John Wheatley for specimen preparation, Allen Higgs for microscope maintenance and Paul Perkes for computer software. The participation of NO was made possible by the Research Experience for Undergraduates Program of the Department of Physics and Astronomy, ASU, with support from the National Science Foundation.

References

Cowley, J. M. (1959). *Acta Cryst.* **12**, 367–375.
Cowley, J. M. (1967). *Prog. Mater. Sci.* **13**, 269–321.
Cowley, J. M. (1976). *Ultramicroscopy*, **1**, 255–262.

Cowley, J. M., Dunin-Borkowski, R. E. & M. Hayward. (1998). *Ultramicroscopy*, **72**, 223–232.
Cowley, J. M. & Moodie, A. F. (1959). *Acta Cryst.* **12**, 423–428.
Cowley, J. M., Spence, J. C. H. & Smirnov, V. V. (1997). *Ultramicroscopy*, **68**, 135–148.
Dunin-Borkowski, R. E. & Cowley, J. M. (1999). *Acta Cryst.* A**55**, 119–126.
Fertig, J. & Rose, H. (1981). *Optik (Stuttgart)*, **59**, 407–429.
Hashimoto, H., Naiki, T. & Mannami, M. (1960). *Fourth International Congress on Electron Microscopy, Berlin (1958)*, Vol. 2, edited by G. Möllenstedt, H. Niehrs & E. Ruska, pp. 331–336. Berlin: Springer-Verlag.
Hirsch, P. B., Howie, A., Nicholson, R. B., Pashley, D. W. & Whelan, M. J. (1965). *Electron Microscopy of Thin Crystals*. London: Butterworths.
Loane, R. F., Kirkland, E. J. & Silcox, J. (1988). *Acta Cryst.* A**44**, 912–927..
Marks, L. D. (1985). *Ultramicroscopy*, **18**, 33–38.
Renard, D., Croce, P., Gandais, M. & Sauvin, M. (1971). *Phys. Status Solidi B*, **47**, 411–421.
Sanchez, M. & Cowley, J. M. (1998). *Ultramicroscopy,* **72**, 213–222.
Van Dyck, D. & Op de Beeck, M. (1996). *Ultramicroscopy*, **64**, 99–107.